Parasite Immunology, 2007, **29**, 501–513 DOI: 10.1111/j.1365-3024.2007.00969.x

Wound healing response is a major contributor to the severity of cutaneous leishmaniasis in the ear model of infection

T. BALDWIN,[1] A. SAKTHIANANDESWAREN,[1] J. M. CURTIS,[1] B. KUMAR,[2] G. K. SMYTH,[1] S. J. FOOTE[3] & E. HANDMAN[1]

[1]The Walter and Eliza Hall Institute, and The University of Melbourne, Australia, [2]Department of Anatomical Pathology, Monash Medical Centre, Australia, [3]The Menzies Research Institute, Australia

SUMMARY

In the conventional mouse model for cutaneous leishmaniasis involving infection with stationary phase Leishmania major *promastigotes at the base of the tail, mice congenic for leishmaniasis resistance loci designated lmr1,2,3 cured their lesions more rapidly and laid down more ordered collagen fibres than the susceptible parental BALB/c mice, while the opposite was the case for the congenic mice carrying the susceptibility loci on the resistant C57BL/6 background. In that model, we showed that wound healing and not T cell responses played a major role in determining the resolution of skin infection. Here, we show a similar disease phenotype in the mouse model that mimics more closely the situation in humans, that is, strictly intradermal infection in the ear pinna with small numbers of metacyclic promastigotes. The data show that at the site of infection the innate and adaptive immune responses act in concert to clear parasites, and induce tissue repair and wound healing. Importantly, the data show that the host responses controlled by the lmr loci, which act locally to control infection in the skin, are distinct from the host responses operating systemically in the draining lymph node.*

Keywords *collagen deposition,* Leishmania*, resistance to infection, wound healing*

INTRODUCTION

The infection of mice with *Leishmania major* has been used as a model to analyse the players of the immune system responsible for lesion cure, as seen in the resistant C57BL/6, or those responsible for disease severity as in the case of the susceptible BALB/c. Murine cutaneous leishmaniasis became the first model to clearly demonstrate the existence of the polarized T cell immune responses with the Th1-type cells producing pro-inflammatory cytokines such as IFN-γ, and the Th2 cells producing IL-4. However, this attractive concept has been shown to be much more complex (1,2). For example, some of our earlier studies examining the disease pattern in mice infected at different sites have shown a variable degree of correlation between the T cell cytokine pattern and severity of disease, depending on the site of infection (3). Similarly, in a genetic cross between susceptible BALB/c and resistant C57BL/6 mice we identified three *L. major* response (*lmr*) loci that control susceptibility to disease caused by infection at the base of the tail (4,5). Congenic mice carrying the susceptibility loci from BALB/c on the genetic background of C57BL/6 (B6.lmr1/2) were more susceptible than the parental C57BL/6, but displayed the same Th1 cytokine pattern as C57BL/6 mice (6,7). Similarly, mice carrying the resistance alleles from C57BL/6 mice on a BALB/c background (C.lmr1/2) were more resistant than BALB/c in the presence of a Th2 cytokine pattern (6,7). The studies described above were carried out using the conventional mouse model of cutaneous leishmaniasis, where the infection used large numbers of stationary phase promastigotes injected at the base of the tail. In the current study, we aimed to examine the effect of the route of infection on the disease pattern and immune responses in the lmr congenic mice using the more natural infection with small numbers of metacyclic promastigotes injected strictly intradermally in the ear pinna (8,9). This model should validate the importance of the susceptibility/resistance loci and the potential applicability to the human disease that is mimicked more closely by this model of infection.

Correspondence: Emanuela Handman, The Walter and Eliza Hall Institute of Medical Research, 1G Royal Parade, Parkville, Victoria 3050, Australia (e-mail: handman@wehi.edu.au).
Received: 6 May 2007
Accepted for publication: 24 July 2007

This study reveals that local and systemic effects are occurring within the congenic mice. At the level of the lymph node, the disease phenotype described for the base of the tail infection was confirmed. Yet, at the site of infection we show that locally, the adaptive immune system appears to work in conjunction with the innate immune system to clear parasites, and induce tissue repair and wound healing. We demonstrate that infection by *L. major* modulates this response in a host-specific manner, with the mouse strains that mount Th1 responses and vigorous wound healing responses also showing resistance to *L. major* lesion development.

MATERIALS AND METHODS

Mice

BALB/c, C57BL/6, C.lmr1/2 and B6.lmr1/2 female mice aged 6–7 weeks were obtained from the specific-pathogen-free animal breeding facility at The Walter and Eliza Hall Institute of Medical Research and maintained in a conventional animal facility. Congenic intervals are on chromosomes 9 and 17. The most proximal and distal markers found to be within the congenic intervals are as follows: B6.lmr1/2, D17Mit57–D17Mit129, D9Mit89–D9Mit71; C.lmr1/2, D17Mit57–D17Mit39, and D9Mit89–D9Mit329 (4).

Parasites

Parasites used were the cloned line V121 derived from the *L. major* human isolate LRC-L137 (MHOM/IL/67/Jericho II) obtained from the WHO Reference Centre for Leishmaniasis, Jerusalem, Israel. Promastigotes were maintained *in vitro* at 26°C in Schneider's *Drosophila* medium supplemented with 10% foetal bovine serum (HyClone, Logan, UT, USA). For infection of mice, the parasites were grown in the biphasic blood agar (NNN) medium (10). In order to maintain virulent stocks of *L. major* for infection purposes, parasites were maintained in CBA/H-nu/nμ mice and cultured *in vitro* for a maximum of 4 weeks.

Infection and monitoring of the disease pattern

For infection, *L. major* V121 metacyclic promastigotes were prepared according to Courret *et al.* (11). Briefly, the primoculture initiated with 5×10^5 logarithmic phase promastigotes per millilitre were grown for 6 days, washed with phosphate-buffered saline (PBS) pH 7·3 before incubation with Peanut Agglutinin (PNA – Vector Laboratories, Burlingame, CA, USA), at a final concentration of 100 μg/mL. After 30 min at room temperature, the agglutinated nonmetacyclic parasites were removed by centrifugation and the metacyclic promastigotes remaining in suspension were washed and resuspended at 10^3/10 μL PBS for injection into mice (8,12).

The mice were anaesthetized with the inhalant anaesthetic methoxyflurane (Medical Development Australia Pty. Ltd) and injected in the pinna of the ear with 10^3 *L. major* V121 metacyclic promastigotes in 10 μL. Ear lesion development was assessed weekly by measuring the diameter of the lesion (13). Lesions were assigned a score from 1 to 4, where 1 represented a small, localized swelling and 4 represented a diameter of 6 mm. Statistical significance, in terms of differences in the rate of lesion development between the congenic mouse strains, was assessed using the 'compareGrowthCurves' function of the statmod software package for R (http://bioinf.wehi.edu.au/software/compareCurves). The initial *P*-values were adjusted for multiple testing using Holm's method.

At 3, 6, 9 and 12 weeks post-infection, the cells from the auricular lymph nodes that drain the injection site and the dermal cells of the ear were analysed for cytokine, and specific RNA production and parasite load as described below. In addition, at 0, 1, 3, 6, 9 and 12 weeks post-infection haematoxylin and eosin (H&E) and Masson's trichrome (MT) staining were done to examine the histopathological events and the degree of collagen deposition occurring in the skin of the ear. The ears from naive and infected mice were removed, fixed in 10% formalin and embedded in paraffin. A 5-μm tissue section was stained with H&E or MT.

Using H&E, we examined the density and composition of the inflammatory infiltrate into the dermis and the onset of chronic inflammation, re-epithelialization of the wound, and the presence of parasites. The degree of inflammation was classified as sparse, moderate or dense based on the area of dermis occupied by the inflammatory cells which was < 20%, 20%–70% and > 70%, respectively.

Masson's trichrome stain was used to determine the amount of collagen deposition and organization in uninfected and infected tissue. In the area of the wound, semi-quantitative assessment of the amount, thickness and ordered distribution of the collagen bundles were documented. Collagen deposition was scored from 0 to 3 using a system common in clinical pathology laboratories, where 0 represents no collagen; 1 corresponds to sparse, irregular collagen deposition; 2 denotes more collagen with some continuity of the collagen bundles; and 3 indicates continuous, parallel alignment of collagen bundle deposition, often with intense staining.

Neutrophil depletion and effect on wound healing

To assess the role of neutrophils during the wound healing process, neutrophils were depleted from parental and congenic mice using 0·5 mg of 1-A8 mAb (a kind gift of Thomas Malek) injected into the peritoneal cavity 24 h prior to infection with V121 metacyclic promastigotes or a

Table 1 PCR primers and expected product sizes of amplified genes

Target	Forward primer	Reverse primer	$MgCl_2$ (mM)	Product size (bp)
PBGD	CCTGGTTGTTCACTCCCTGA	CAACAGCATCACAAGGGTTTT	3	98
IL-4	TTTTGAACGAGGTCACAGGA	AGCCCTACAGACGAGCTCAC	3	107
IFN-γ	CTTCTTCAGCAACAGCAAGG	TGAGCTCATTGAATGCTTGG	3	101
FIZZ1	TCCCTCCACTGTAACGAAGAC	AGGCAGTTGCAAGTATCTCCA	3	153
MRC1	TGCAAAGCTATAGGTGGAGAGC	ACGGGAGAACCATCACTCC	3	165

full skin punch wound. Control mice were injected with the isotype control antibody GL117. Infected mice were monitored weekly for lesion development as described.

The neutrophil numbers in the circulation were monitored on daily blood smears for the first 14 days to establish when levels had returned to baseline and then at week 5 of infection. Blood films were stained with May Grunwald–Giemsa before counting using microscopy.

For the full skin punch wound, mice were anaesthetized with Xylazil/Ketamil (0·03 g/0·01 g/kg bodyweight) before a 4-mm punch (Stiefel Laboratories SFM, Germany) biopsy was taken at the base of the tail. The wound healing process was monitored by measuring the diameter of the lesion on days 0, 1, 3, 5 and 7 post-punch and histopathological examination of skin taken from the wound edge and stained with H&E. The statistical test used to compare the kinetics of wound closure for punch biopsies is described at (http://bioinf.wehi.edu.au/software/russell/perm/help.html). Using microscopy, the H&E stained sections acquired from two mice at each time point were examined to determine the density of inflammation and type of inflammatory cells present.

Limiting dilution analysis of parasite load in the cells of the lymph node and skin

At designated time points, draining lymph nodes from two mice in each group were taken for analysis. The parasite burden was determined by limiting dilution analysis as described (3). The parasite burden is expressed as the number of organisms per lymph node.

At weeks 3, 6, 9 and 12 post-infection, the ears were removed and processed to determine the parasite load and cytokine level in the skin. To measure the parasite load in the skin, isolated ears were surface sterilized before separating the dorsal sheet from the ventral one. This was floated onto 500 μL of 0·25% Trypsin, 1 μM ethylenediamine tetra-acetic acid (EDTA, Gibco-BRL, NY, USA) for 30 min at 37°C, 10% CO_2. After incubation, cells were flushed from the split surface of the ear explant using medium and then passed through a 40 μm cell strainer (Millipore, Hertfordshire, UK). Cell viability and counts were completed using 1 μg/mL ethidium bromide and acridine orange in PBS (14,15), and limiting dilution analysis was carried out. The parasite burden is expressed as the number of organisms per ear pinna. The lymph node or skin cells not used for parasite burdens were processed for the analysis of cytokine production as described below.

Cytokine and alternatively activated macrophage gene expression

Analysis of the classic macrophage IL-4 and IFNγ mRNA expression and examination of genes expressed specifically by alternatively activated macrophages Found in Inflammatory Zone (FIZZ1) and Mannose Receptor C type 1 (MRC1) was carried out using the real-time fluorescence PCR assay described by Elso *et al.* (6). Real-time fluorescence PCR assays were carried out on the LightCycler (Roche Molecular Biochemicals, Basel, Switzerland) using the Faststart DNA Master SYBR Green kit (Roche Molecular Biochemicals) with the primers for IL-4, IFNγ, FIZZ1, MRC1 and the housekeeping gene porphobilinogen deaminase (PBGD) (6,16). This housekeeping gene was chosen because it is a single-copy gene with no pseudogenes, and it is expressed at low levels similar to cytokine expression. HPLC-purified primers were obtained from Integrated DNA Technologies. The primers, conditions and expected product size are listed above (Table 1).

The PCR conditions were: 10 min at 95°C followed by 45 cycles of 10 s at 95°C, 5 s at 60°C and 5 s at 72°C.

RESULTS

Effects of the host response loci on the course of disease

The parental and congenic mice were inoculated intradermally with 10^3 *L. major* V121 metacyclic promastigotes in the pinna of the ear. As shown in Figure 1, using the diameter of the developing lesion as a marker for the degree of susceptibility to disease, the mice can be ordered from the most susceptible to the most resistant. Thus, BALB/c > C.lmr1/2 > B6.lmr1/2 > C57BL/6.

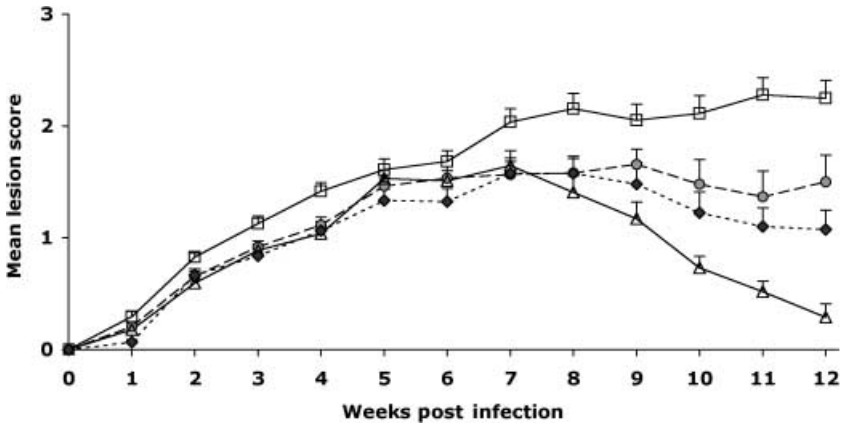

Figure 1 The disease pattern in BALB/c, C.lmr1/2, C57BL/6 and B6.lmr1/2 mice infected intradermally in the ear with 10^3 *Leishmania major* V121 metacyclic promastigotes. The mean lesion scores and SE of the mean are shown as a function of time. Data was pooled from four experiments, 30–42 mice per group – (□) BALB/c (●) C.lmr1/2 (△) C57BL/6 and (◆) B6.lmr1/2.

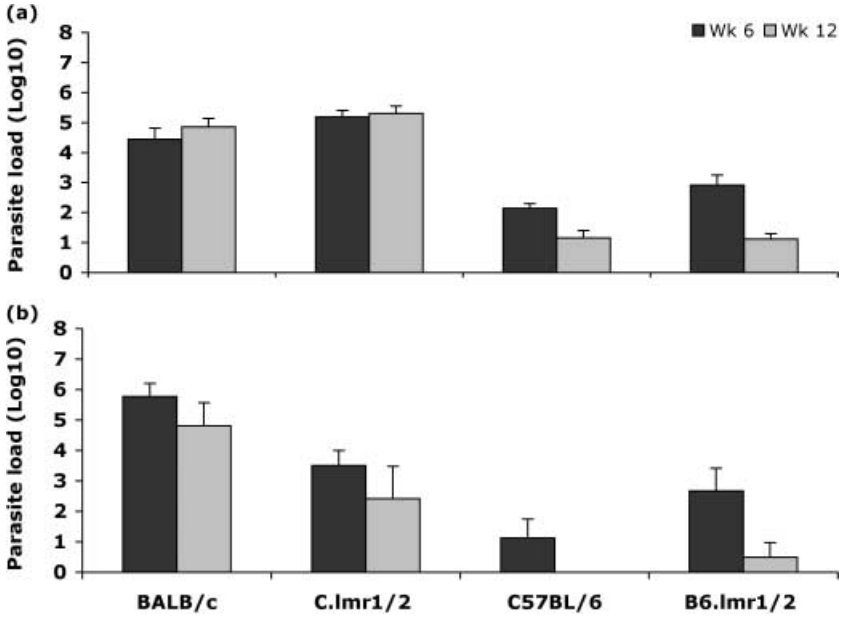

Figure 2 The mean parasite load and SE of the mean per lymph node or ear. Cells isolated from the auricular draining lymph node or skin of the ear 6 and 12 weeks after infection with 10^3 *Leishmania major* V121 metacyclic promastigotes in the ear pinna of BALB/c, C.lmr1/2, C57BL/6 and B6.lmr1/2 mice. Data collated from seven mice per sample group. (a) Lymph node and (b) skin of ear.

Statistical significance between the curves in Figure 1 was assessed using a permutation test developed to compare groups of growth curves. The test was applied to the lesion scores over the period of the experiment when the contribution of the different *lmr* loci to susceptibility was most apparent, that is, weeks 8–12 post-infection. All pair-wise comparisons between the mouse strains were statistically significant ($P = 0{\cdot}0000$–$0{\cdot}012$, $n = 24$–36), except for that between B6.lmr1/2 and C.lmr1/2 ($P = 0{\cdot}36$, $n = 24$–33), confirming the conclusions reached by visual inspection of Figure 1.

Relationship between the disease pattern and parasite burden

The size of the lesion developing at the site of infection may reflect the parasite burden or the degree of tissue damage caused by the host immune response to the parasite. Here, we set out to quantify the parasite burden at weeks 6 and 12 post-infection at the site of infection (ear pinna) and in the lymph nodes draining the lesion and to determine the correlation with the size of the lesion.

In the susceptible parental BALB/c and C.lmr1/2 congenic mice, there was no difference in the parasite burden in the draining lymph node during the course of infection (Figure 2a). The parasite load in the lymph nodes was high in both strains, possibly reflecting the similar size of the lesions. In contrast, the C57BL/6 mice showed a much lower load even at week 6, which is the peak of lesion size (Figures 1 and 2a). The parasite load declined further between weeks 6 and 12 as the mice healed their lesions (Figure 2a). The parasite load of the congenic B6.lmr1/2 mice was somewhat higher than the C57BL/6 mice at week

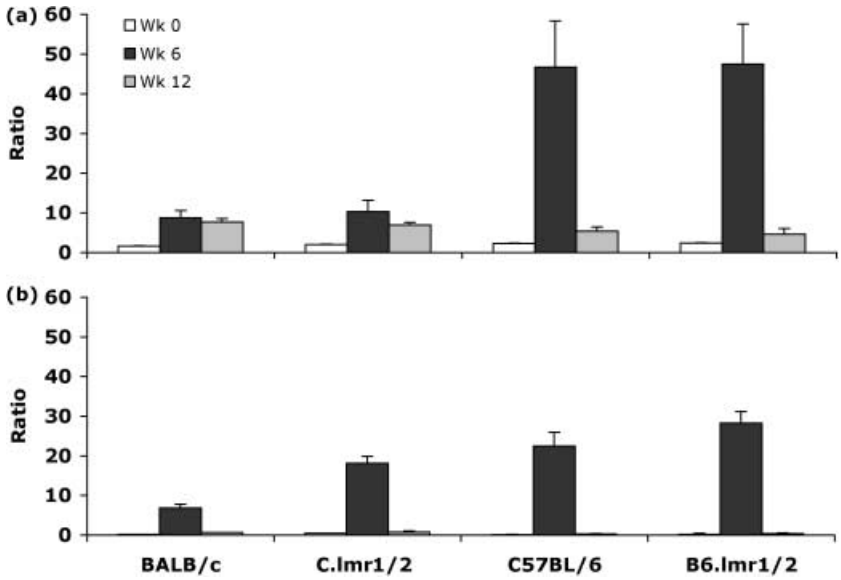

Figure 3 Mean IFN-γ : IL-4 cytokine ratio detected in naïve, and infected parental and congenic mice 0, 6 and 12 weeks post-infection with 10^3 *Leishmania major* V121 metacyclic promastigotes. Data collated from 10 to 12 mice per sample group. (a) Lymph node and (b) skin of ear.

6, but low and similar to the parental mice at week 12 despite the difference in lesion size.

In conclusion, in BALB/c and C57BL/6, the parasite load in the lymph node appeared to reflect the state of their lesions. In contrast, in the case of the congenic mice, the parasite load did not reflect the severity of their disease. Thus, despite the fact that the C.lmr1/2 mice had smaller lesions than the BALB/c mice and B6.lmr1/2 mice had larger lesions than C57BL/6 mice, the parasite burdens in the lymph nodes of the congenic mice were similar to the parental load.

In contrast to the situation in the draining lymph nodes, the examination of the parasite burden in the ears of the congenic mice showed a good correlation with the state of the lesion, and thus, disease severity. As in the case of the draining lymph node, the susceptible BALB/c mice had the highest parasite load in the skin (Figure 2b), which persisted throughout the course of infection. The C.lmr1/2 mice had a somewhat lower parasite load at week 6 post-infection, and this declined further at week 12. The peak parasite load of the C57BL/6 was at 3 weeks (data not shown) long before the peak of the lesion size (Figure 1) and it declined to a very low parasite number by week 6. Parasites were not detectable at week 12 reflecting the healing of the lesions. In the case of the congenic B6.lmr1/2, the parasite burden in the skin was significantly higher than the C57BL/6 mice at week 6 and unlike the parental C57BL/6 mice, parasites were detected in the B6.lmr1/2 mice at week 12 post-infection (Figure 2b). Thus, in contrast to observations in the lymph nodes, in the skin the C.lmr1/2 and B6.lmr1/2 congenic lines presented parasite loads that were different from the parental mice and reflected more the phenotype of their lesions.

Relationship between the disease pattern and the cytokine profile

In parallel with the analysis of parasite load, we examined the cells of the ear pinna and draining lymph node for the presence of mRNA encoding the signature Th1 and Th2 cytokines IFN-γ and IL-4. The level of cytokine mRNA in the various mouse strains was quantified using real-time fluorescence PCR before infection and at weeks 6 and 12 post-infection, and expressed as the mean ratio of IFN-γ : IL-4 (Figure 3a,b).

Figure 3a shows that for the cells in the draining lymph node prior to infection, the ratio of IFN-γ : IL-4 was approximately 2. At 6 as well as 12 weeks post-infection, there was no difference in the ratio of IFN-γ : IL-4 between the parental and the congenic mice of all genotypes. However, this ratio was only about 6 in the case of the BALB/c and the congenic C.lmr1/2, but it was over 40 in the case of C57BL/6 and B6.lmr1/2 (Figure 3a). By week 12, all groups showed a low ratio of IFN-γ : IL-4, similar to the control uninfected mice, irrespective of their lesion size.

The data indicated that in the lymph node, during most of the infection, the C.lmr1/2 and B6.lmr1/2 congenic mice had a similar cytokine ratio to the parental mice and this showed no correlation with the severity of their lesions.

In the skin of the uninfected mice of all genotypes, the IFN-γ : IL-4 ratio was 1 (Figure 3b). At week 6 after infection, the C.lmr1/2 had significantly higher ratios of IFN-γ : IL-4

Journal compilation © 2007 Blackwell Publishing Ltd, *Parasite Immunology*, **29**, 501–513

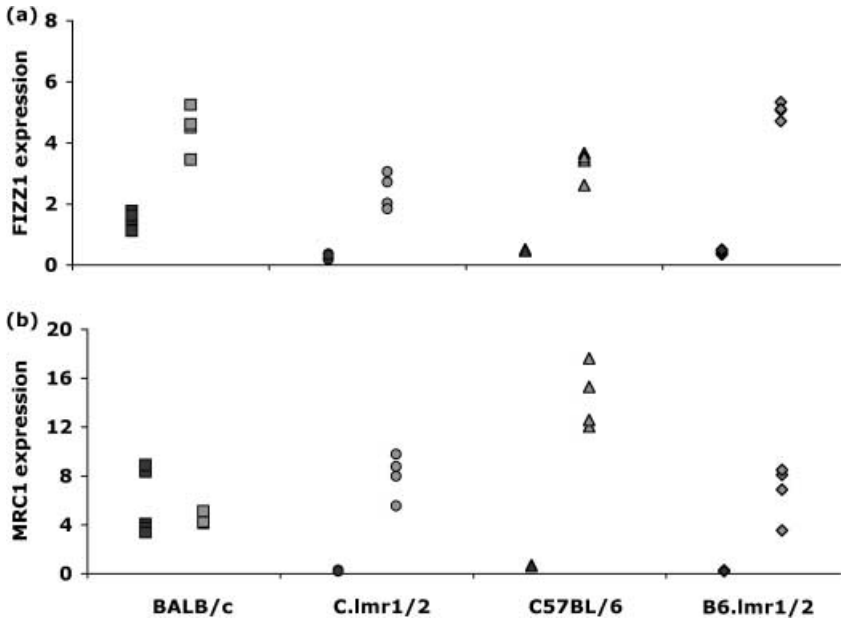

Figure 4 Infected : naive ratio of mRNA encoding the alternatively activated macrophage markers detected in the skin of parental and congenic mice, 6 and 12 weeks post-infection with 10^3 *Leishmania major* V121 metacyclic promastigotes. Data collated from 4 to 6 mice per sample group – (dark grey shading) week 6 and (light grey shading) week 12. (a) FIZZ1 and (b) MRC1.

than the BALB/c parents. In contrast, there was no difference between the congenic B6.lmr1/2 and the parental C57BL/6 mice (Figure 3b). However, the C57BL/6 and the congenic B6.lmr1/2 had IFN-γ : IL-4 ratios similar to those in C.lmr1/2 mice, but higher than the susceptible BALB/c. By week 12, all groups had returned to baseline levels (Figure 3b).

In contrast to the situation in the lymph nodes, the BALB/c and C.lmr1/2 congenics at week 6 showed a correlation between the cytokine pattern in the skin and the severity of subsequent disease. Surprisingly, at week 12 post-infection, when the difference in disease severity is most pronounced the C.lmr1/2 and B6.lmr1/2 congenic mice had IFN-γ : IL-4 ratios in the skin that were comparable to their parents.

Alternatively activated macrophages

In view of the role of alternatively activated macrophages in wound healing and collagen deposition, we explored the expression of specific genes of the alternative macrophage activation pathway in the skin and draining node. We examined the cells of the ear pinna and draining lymph node for the presence of mRNA encoding specific markers for the alternatively activated macrophage genes, FIZZ1 and MRC1. The level of mRNA in the various mouse strains was quantified using real-time fluorescence PCR before infection and at weeks 6 and 12 post-infection, and expressed as the mean ratio of FIZZ1 or MRC1 in cells from infected to naive mice (Figure 4a,b). Notably, only data from skin samples have been included because the lymph node expression was negligible in all cases making these ratios 1 : 1.

Figure 4a shows that at week 6, the ratio of FIZZ expression in infected vs. naïve cells in the BALB/c is approximately 1–1·5, whereas in the C57BL/6, C.lmr1/2 and B6.lmr1/2 expression is two to three times lower. By week 12, all ratios had risen with the BALB/c and B6.lmr1/2 having the highest expression of 3·5–5·2 : 1 and 4·7–5·1 : 1, respectively. The C57BL/6 expression was between 2·6 and 3·7 : 1 whilst the C.lmr1/2 had the lowest ratio of 1·8–3 : 1.

At week 6, the ratio of MRC expression in infected to naïve cells is 5·3–14 times higher in the BALB/c compared to the C57BL/6 parental mice and the congenic groups, respectively (Figure 4b). However, by week 12 there appears to be a complete shift with the highest infected to naïve ratio ranging from 12 to 17·6 : 1 in the C57BL/6, followed by 5·6–9·8 : 1 in the C.lmr1/2, 3·5–8·5 : 1 in the B6.lmr1/2 and the ratios of 4·2–5 : 1 observed in the BALB/c parental mice.

The expression of the specific mRNA markers suggests that the susceptible BALB/c have elevated levels of alternatively activated macrophages present during the early stages of infection compared with the C57BL/6, C.lmr1/2 and B6.lmr1/2. However, this balance shifts during the later stages of infection with the resistant C57BL/6 having the greatest overall expression of alternatively activated macrophages followed by the congenic groups and finally the BALB/c.

Density of inflammation in the skin of the parental and congenic mice

The recruitment of inflammatory cells to the wound plays an important role in the resulting cellular processes that lead

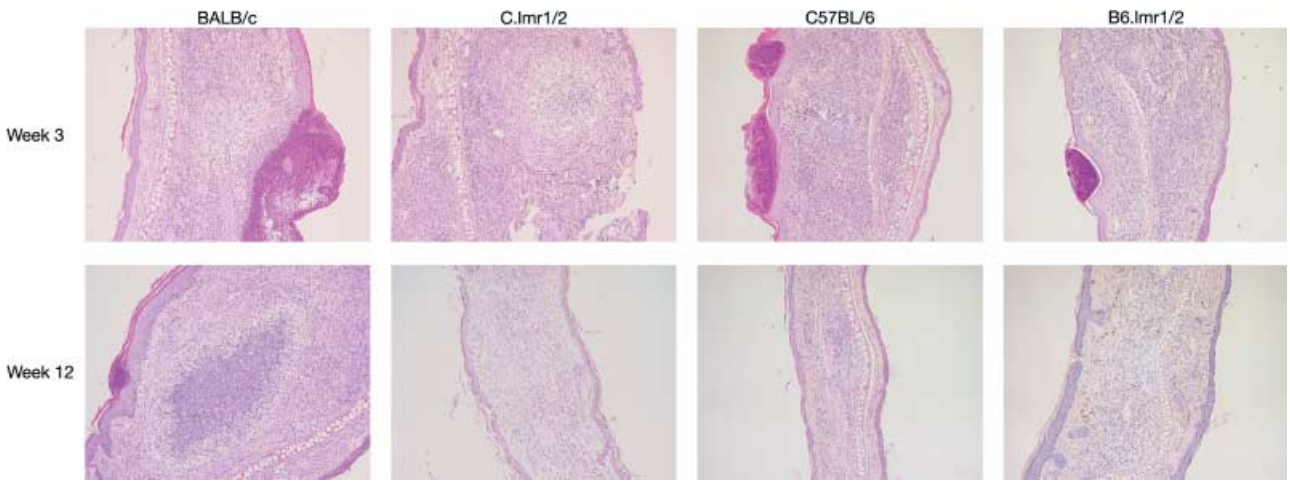

Figure 5 Inflammation – H&E stained skin tissue sections from weeks 3 and 12 post-infection with 10^3 *Leishmania major* V121 metacyclic promastigotes. At week 3, all four strains showed a wound with an inflammatory exudate on the surface, the BALB/c showing the largest wound. There was moderate to dense dermal inflammation in all four strains. At week 12, all four strains showed re-epithelialization with the BALB/c still showing an inflammatory exudate on the surface. The dense inflammation persisted in BALB/c, but the C.lmr1/2 and B6.lmr1/2 had sparse inflammation and the C57BL/6 had negligible inflammation. All tissue sections are at ×100 magnification.

to tissue remodelling and healing. Using H&E stained sections from naïve and infected mice at 1, 3, 6, 9 and 12 weeks post-infection, we determined the degree of inflammation in the ear. The inflammatory and associated cell populations detected at the site of infection included neutrophils, macrophages, lymphocytes, fibroblasts and eosinophils (data not shown). The density of inflammation was quantified by measuring the area occupied by the inflammatory cells and was classified as sparse, moderate or dense. One week after infection, the cell populations in all strains of mice appeared very similar to the naïve specimens as described by Belkaid *et al*. (9) for this quiescent stage during the early phase of infection. Over the subsequent 3 weeks, the density of the inflammation increased to moderate levels in the C57BL/6 and B6.lmr1/2 and dense inflammation in the BALB/c and C.lmr1/2 mice (Figure 5).

As the disease progressed, the degree of inflammation, the proportion of each inflammatory cell type present and the ability to clear parasites began to vary between the mouse strains. In the C57BL/6, lymphocyte and macrophage numbers were consistently greater than neutrophils throughout the course of the experiment. In these mice, neutrophil numbers as a marker of acute inflammation were reduced at week 6 and absent at weeks 9 and 12. This correlated well with the rapid drop in parasite numbers and the decline in the density of inflammation to negligible by week 12 (Figure 5) when the lesions had healed. Fibroblasts were observed at all time points, but were most abundant at weeks 6, 9 and 12 as the number of inflammatory cells decreased. In contrast, in BALB/c the inflammation was sustained throughout (Figure 5). In these mice, the combined lymphocyte and macrophage numbers were similar to the neutrophils at all time points. Parasites and neutrophils were still visible at week 12 reflecting acute inflammation and active infection. In BALB/c mice, few fibroblasts were observed within the lesion site. In the case of the congenic mice, both the C.lmr1/2 and B6.lmr1/2 mice had moderate/sparse inflammation (Figure 5), with low parasite and neutrophil numbers in the lesion at week 12. Throughout the period of observation in the B6.lmr1/2, the number of macrophages and lymphocytes was greater than the neutrophil numbers. This was also the case for the C.lmr1/2 mice at week 12 post-infection. The totality of the data indicate that lesion healing and clearance of parasites from the skin correlates with the presence of greater numbers of chronic rather than acute inflammatory cells within the tissue.

Using the degree of inflammation and clearance of parasites as a tool to assess local healing, the strains can be ordered from most dense degree of inflammation to least dense: BALB/c > C.lmr1/2 > B6.lmr1/2 > C57BL/6. This ranking mirrors the ranking for the degree of susceptibility to disease as measured by lesion size.

Re-epithelialization in the skin of the parental and congenic mice

The formation of granulation tissue in an open wound allows the re-epithelialization phase to take place, with the migration of epithelial cells across the new tissue to form a barrier between the wound and the environment. Skin closure

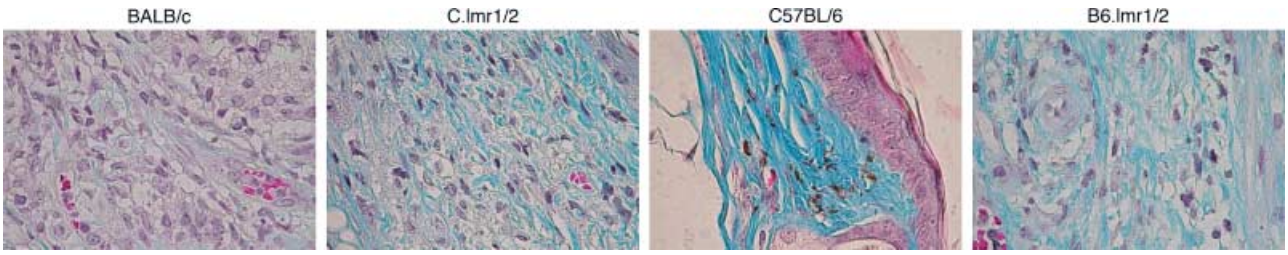

Figure 6 Histological sections of the parental and congenic skin at week 12-post-infection with *Leishmania major* V121. Tissue stained with Masson's trichrome shows strain-dependent deposition of collagen fibres which included sparse, disorganized collagen bundles in the BALB/c, thick highly organized collagen bundles in C57BL/6 and thick yet disorganized collagen bundles in the congenic strains. All tissue sections are at ×100 magnification.

was observed in the C57BL/6 mice at all experimental time points examined (Figure 5). Similarly, the C.lmr1/2 and B6.lmr1/2, with the exception of a single mouse at weeks 6 and 9, respectively, also showed restoration of the skin barrier (Figure 5). In contrast, the epithelial tissue in the BALB/c mice took longer to restore this barrier with closure occurring between weeks 6 and 12 post-infection (Figure 5), reflecting the increased severity of the lesions.

Collagen deposition in the skin of the parental and congenic mice

Our earlier study using the base of the tail model of infection showed that differences in wound healing played a critical role in the functional differences in susceptibility between the congenics and their parental lines (16). We used the MT staining for collagen as a measure of wound healing to examine the ear skin in naïve and infected mice over the 12 weeks of infection. We observed strain-specific differences in the deposition of collagen fibrils (Figure 6) with the biggest differences during weeks 9–12 which coincide with the greatest difference in lesion size.

In the naïve mice and 1 week after infection of all strains, collagen was evenly distributed, showed great depth and the collagen bundles were aligned in an ordered parallel configuration with fibroblasts being the only cell type present (data not shown).

The C57BL/6 mice showed thick but not well-ordered collagen bundles at the early 3-week time point and these became well ordered by week 12 after infection, by which time the majority of lesions had healed (Figure 6). In contrast, in the BALB/c parental strain, sparse, thin, unorganized collagen bundles were observed in the active regions of the wound (Figure 6). In general, the fibres remained thin and lacked organization at the wound site throughout the infection period (Figure 6). In contrast to the parental BALB/c mice, in the C.lmr1/2 mice, thick collagen bundles were observed from week 9 onwards. By week 12, the C.lmr1/2 skin consistently had more collagen than the BALB/c mice, but less than the C57BL/6 donor (Figure 6). In the B6.lmr1/2, collagen bundles were seen at week 6 (data not shown) and continued to be present throughout the period of observation. However, throughout the infection including week 12, the B6.lmr1/2 had less collagen in the lesions and these were less organized compared to the C57BL/6 parental mice (Figure 6).

Using the collagen score as a marker for wound healing capability, the mice can be ranked from the slowest to the fastest as follows: BALB/c > C.lmr1/2 > B6.lmr1/2 > C57BL/6. This ranking is identical to that observed for disease/lesion phenotype indicating that the same processes that control wound healing also act in the infectious lesions.

Neutrophil numbers in the parental and congenic mice

Neutrophils are known to be the first leucocytes that migrate to the site of infection or wounded skin. It has long been debated whether the presence of neutrophils is beneficial or detrimental to the wound healing process and specifically whether they prevent or promote infection with *L. major*. Here, we set out to establish whether there were differences between the baseline neutrophil levels of the parental and congenic groups and how these differences may impact upon the wound healing process following infection with *L. major*.

The baseline neutrophil numbers as a percentage of the total white blood cell number in the blood of C57BL/6 and their congenic B6.lmr1/2 were similar at $11{\cdot}6 \pm 0{\cdot}8$ and $8{\cdot}9 \pm 0{\cdot}7$ ($n = 20$). In contrast, their percentage in BALB/c mice was $21{\cdot}5 \pm 1{\cdot}4$ ($n = 20$) and $35{\cdot}7 \pm 1{\cdot}7$ ($n = 20$) for the C.lmr1/2 congenic mice (Figure 7a).

Skin punch biopsies and infection with *L. major* were performed on neutrophil depleted and control mice to determine whether the difference in neutrophil numbers between the susceptible and resistant mice influenced pathogenicity and wound healing. At days 0, 1, 3, 5 and 7

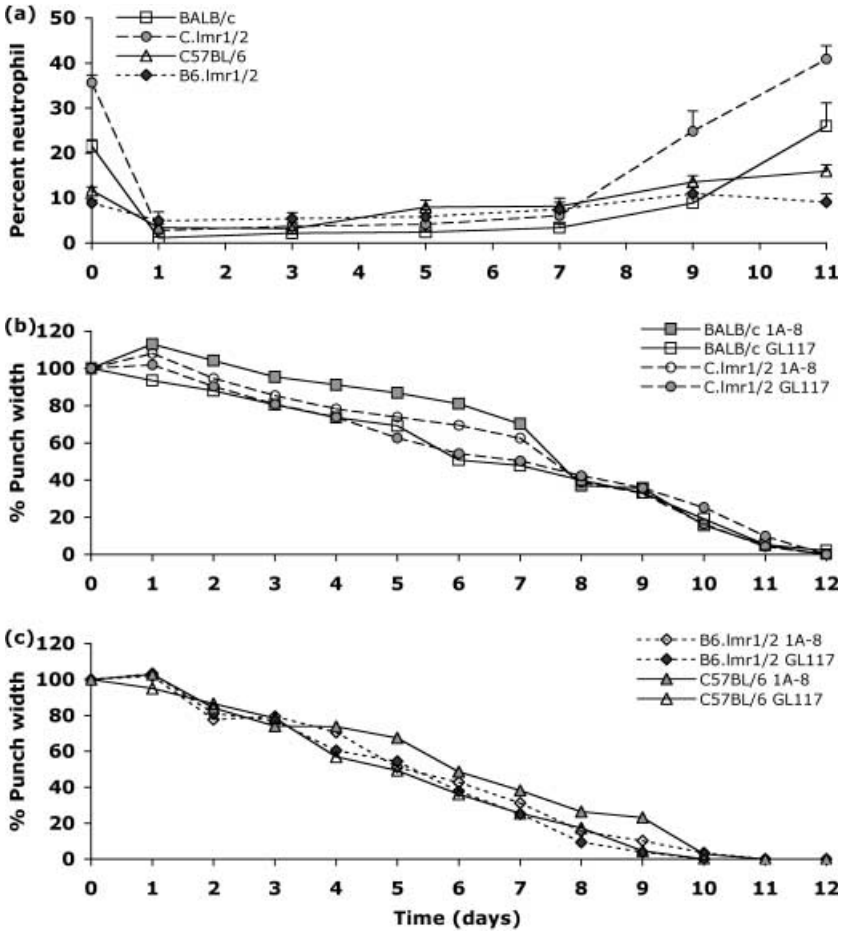

Figure 7 The baseline neutrophil levels as the percent of the total white blood cells and the time taken for re-establishment of the neutrophil numbers after depletion with mAb 1-A8, in both the punch biopsy and *Leishmania major* infection experiments. Data was pooled from three experiments, 20 mice per group (a); wound closure expressed as mean percent of punch width after a full 4-mm skin biopsy in neutrophil depleted and control mice. Data collated from five mice per group in either BALB/c and C.lmr1/2 (b), and/or C57BL/6 and B6.lmr1/2 (c).

post-biopsy tissue was taken from around the edge of the wound to assess the level of inflammation and the types of inflammatory cells present.

The time taken for re-establishment of basal neutrophil numbers in the circulation after depletion varied between the mouse strains, in both the punch biopsy and infection experiments (Figure 7a). The C57BL/6 and B6.lmr1/2 neutrophil levels returned to normal by day 8, whilst the BALB/c and C.lmr1/2 reached normal levels around day 10, possibly a reflection of the greater number of neutrophils to be produced in the bone marrow. However, there were no long-term differences in the numbers of neutrophils between the depleted and control mice in any of the treatment groups.

Examination of the H&E stained histopathological sections revealed that the degree of inflammation in the neutrophil depleted groups was only marginally different compared to that of the control groups and the inflammation was classified as moderate in all groups (20%–70%) (data not shown). Since the inflammation was similar in the presence or absence of neutrophils, the composition of the inflammatory cells occupying that space in the depleted mice shifted from an acute towards a chronic inflammatory cell mix, which could potentially lead to faster healing. Consistent with this possibility is our observation of a bias in the inflammatory cell profile in the dermal tissue of the control resistant C57BL/6. In these mice at days 5 and 7 after punch biopsy the dermal tissue was primarily occupied by macrophages, lymphocytes and fibroblasts, and the chronic inflammatory cells whereas the susceptible BALB/c mice still contained an acute inflammatory cell mix which included large numbers of neutrophils.

In the punch biopsy experiment (Figure 7b,c), at 24 h the wound diameter of all control mice was similar to the initial diameter (93·5%–103% of the initial diameter on day 0), whilst the neutrophil depleted mice had somewhat larger wound diameters ranging from 103% to 113% of the original diameter. Interestingly, the macroscopic appearance of the wound was also different. The neutrophil depleted mice had a wound circumference that looked identical to the punch shape, and was circular and smooth with no attachment of the

skin and muscular layer, whereas the wound circumference of the control group appeared irregularly shaped with adhesion of the skin and muscular layer. During the wound healing process the neutrophil depleted mice maintained the circular, smooth wound edge whilst the controls became more and more irregularly shaped throughout the time course. The mechanism by which the absence of neutrophils within the inflammatory exudate in the wound causes these changes is yet to be determined.

By day 2 (Figure 7c), the width of the C57BL/6 and B6.lmr1/2 control wounds had decreased by 20%, with wound size continuing to diminish by about 10% per day with complete healing observed on day 10. The wounds in BALB/c and C.lmr1/2 control mice followed a similar, but slower pattern of healing with a rate of closure of 5%–8% per day with complete closure on day 12 (Figure 7b). The faster healing observed in the C57BL/6 and B6.lmr1/2 validates the importance of the early shift from an acute to a chronic inflammatory cell infiltrate described above. In the parental and congenic mice that had their neutrophils depleted, the day of wound closure was similar to the control mice (Figure 7b,c). The wound diameter in the neutrophil depleted mice was somewhat larger than the controls at the 24 h time point suggesting that the healing rate of the 1-A8 treated groups was marginally faster than the controls.

Despite the differences described above, statistical analysis indicates that there was no significant difference between the punch biopsy healing rates of the control and neutrophil depleted mice suggesting that neutrophils do not play a major role in the kinetics of the wound healing process. Moreover, there was also no difference in the lesion development between the neutrophil depleted and control parental and congenic mice infected with *L. major* (data not shown), indicating that the presence of neutrophils during the early stages of infection does not influence the long-term outcome of infection.

DISCUSSION

The model of murine cutaneous leishmaniasis is a very attractive system to examine the contribution of the host genetics to susceptibility to disease because of the availability of resistant and susceptible strains of mice. In earlier studies, we identified three genetic loci designated *lmr1–3*, which determine the severity of disease in mice infected with *L. major* at the base of the tail (4,5). In that model, we showed that disease susceptibility, as measured by the size of the lesion, was not linked to T cell immune responses (6,7), but depended significantly on the ability of the mice to heal skin wounds (16), suggesting a role for the innate immune system.

A significant concern about drawing conclusions about susceptibility to disease from a single infectious model arose from the surprising observation made in our laboratory that in different strains of inbred mice, the site of infection determines to a large extent the severity of disease (3). Therefore, we initiated the current study to examine the importance of the three genetic loci, *lmr1–3* for disease severity in the ear model of infection, which is more similar to the situation in humans (8,9).

In the current study, we injected small numbers of metacyclic *L. major* V121 promastigotes intradermally into the ear pinna of the reciprocal congenic lines, carrying either all the susceptibility or all the resistance alleles. Throughout the 12 weeks of infection, we compared the disease pattern, the parasite loads, and the local and systemic cytokine responses in the congenic and parental mice. We also examined the local inflammatory and wound healing responses occurring in the ear skin during infection.

The disease pattern of the parental susceptible BALB/c and resistant C57BL/6 mice followed the well-documented phenotype described for the footpad, base of tail and the ear models by colleagues and our own laboratory (3,4,8). However, the resistant or susceptible phenotypes became apparent somewhat later in infection, probably due to the slower lesion development in the ear compared to other sites. In the congenic mice, the mean lesion scores were intermediate between the two parental extremes. Using lesion size as the criterion for resistance or susceptibility, C.lmr1/2 was clearly more resistant than the parental BALB/c whilst the B6.lmr1/2 was more susceptible than the C57BL/6. These results confirmed that the presence of the donor interval significantly affects the speed of lesion healing in both congenic directions, although it is still clear that the disease phenotype is controlled by multiple genes, not all of them present on the *lmr* loci. Another advantage of this model is that it presents a clearer disease pattern than that obtained previously using the base of the tail as the site of infection.

This study also confirms the importance of wound healing in resistance to *L. major* infection in the more natural low parasite dose model of ear infection. Thus, the susceptibility-conferring BALB/c *lmr* loci slowed down the wound healing on the C57BL/6 background, and the resistant C57BL/6 loci accelerated healing on the BALB/c background, implicating the presence of controlling genes within the congenic intervals.

In order to get a true gauge of whether the degree of tissue damage (lesion size) was due to the number of parasites or the host immune response to infection, we quantified the parasite burden in the draining lymph node and ear. In the lymph node, the parasite load for the parental BALB/c and C57BL/6 correlated well with the severity of disease. A high lesion score corresponded to a high parasite load and vice

versa for a low lesion score. Surprisingly, this was not the case in the congenic lines where the parasite load in the lymph nodes was similar to the parental line, despite distinctly different lesion size. The picture was quite different when the parasite load in the ear was measured and compared to the lesion scores. In the skin, the parasite burden correlated well with the severity of disease for all groups of mice. This suggests that the genes involved in wound healing are also important for parasite clearance, but they exert a local and not a systemic effect. Additional and distinct mechanisms causing susceptibility or resistance to infection must operate at the level of the lymph node.

In view of the difference in parasite clearance between the skin and lymph nodes, we also examined the cytokine responses occurring at both sites. Cytokine expression has long been used as an indicator of the type of T-cell response induced by infection. Thus, IL-4 expression has been used as an indicator of a Th2 type response and implicated in disease exacerbation, as seen in the susceptible BALB/c mice, whilst elevated IFN-γ levels have been associated with a Th1 type response and resolution of disease as in the resistant C57BL/6 mice (1).

Throughout the period examined, we found that the ratio of IFN-γ : IL-4 mRNA extracted from the draining lymph nodes of the congenic mice mirrored that of the parental mice. These results indicated that the congenic mice, while differing in disease severity from their parental strain, displayed systemically the characteristic T helper type cytokine response of the parent. This is in agreement with the data obtained in the conventional model of tail infection (6,7). In contrast to the situation in the lymph nodes, in the skin of the C.lmr1/2 mice, which are more resistant than the parents, the ratio of IFN-γ : IL-4 mRNA was more similar to that of the resistant C57BL/6 mice than to the parental BALB/c. This was most apparent at 6 weeks post-infection before the start of lesion cure and it may be predictive of the ability of the mice to cure. However, this phenomenon was not observed in the case of the B6.lmr1/2 mice, where there was no difference between the congenic and parental C57BL/6 mice. In addition to the examination of the IL-4 levels as a marker of Th2 type responses, we examined the level of IL-10 mRNA transcripts and found no difference in the lymph node and skin between the parental and congenic mice (data not shown). Interestingly, the level of cytokine mRNA and presumably cytokine activity in the skin was always lower than that detected in the draining lymph nodes.

In the skin, the parasite burden and cytokine response correlated well with the severity of disease for all groups of mice. While T cell responses through their cytokines are important, in this mouse model they are independent of wound healing and they are, most likely, not the initiating factors determining disease severity. Our earlier studies (6,7) have shown that there is no difference between the susceptible and resistant mice in the cytokine pattern during the first 24–48 h post-infection, a time when wound-healing mechanisms are already active. Moreover, our data also show that there is no difference between wild type C57BL/6 and hypothymic nude C57BL/6 mice in wound closure after skin punch biopsy (data not shown), indicating that T cells do not contribute significantly to this process.

Since the skin data suggested that a localized effect was controlling the wound healing process, we examined more closely the mechanics of healing. By quantitating the inflammatory cells present in the skin during the infection, the parasite clearance, re-epithelialization and collagen deposition, we were able to detect differences between the susceptible and resistant mice after the initial quiescent period documented by Belkaid *et al.* (9). Wound healing is a dynamic continuum with overlapping but distinct processes of inflammation, proliferation and tissue remodelling where cells of the innate immune system such as neutrophils arrive first followed by macrophages, lymphocytes and finally fibroblasts (17). In the *Leishmania*-induced lesion, acute inflammation as reflected by the presence of neutrophils seems to correlate with active and prolonged infection and delayed recruitment of lymphocytes and fibroblasts, as well as delayed collagen deposition. Collagen deposition and wound healing seemed to correlate with a shift from acute inflammation with numerous neutrophils to a more chronic infiltrate of macrophages, lymphocytes and fibroblasts. Collagen deposition was only prominent in areas where re-epithelialization had occurred, parasites had been cleared and inflammation was controlled.

In the BALB/c, the nonhealing state of the lesion corresponded with the inability of the inflammatory phase to move from the acute to the chronic cell infiltrate. It appears that as long as neutrophils in the lesion outnumbered the lymphocytes and macrophages wound healing could not be orchestrated, although the neutrophils *per se* are not critical to the disease phenotype. Despite the large variation in the baseline numbers of neutrophils present in the different mouse strains it appeared from the punch wound and infection experiments that the neutrophils do not play a major role in the kinetics of the wound healing process. Although neutrophils have been reported to impair the re-epithelialization process (18) our data show that C.lmr1/2 mice which have the largest number of neutrophils re-establish the epithelial layer to the same extent as the other mouse strains.

We examined the recruitment of classic or alternatively activated macrophages to the skin because there is evidence that macrophages release growth factors and cytokines that not only play a pivotal role in parasite killing and clearance but also mediate subsequent stages of fibroplasia and formation of granulation tissue that are essential for wound

Journal compilation © 2007 Blackwell Publishing Ltd, *Parasite Immunology*, **29**, 501–513

repair and new tissue development (19,20). Our data suggest that the presence of elevated numbers of alternatively activated macrophages during the early stages of infection may be detrimental, thus contributing to susceptibility to *L. major* as described for the BALB/c mice (21 and this manuscript). However, a greater number of alternatively activated macrophages during later stages as observed in the C57BL/6 and congenic lines appears advantageous to tissue re-modelling when their association with fibroblasts is likely to be occurring (19,20). Our data suggest that in the susceptible BALB/c it is not the presence of neutrophils that dictates the healing process, but rather the inadequate recruitment of chronic inflammatory cells into the wounded tissue. Whether, during early stages, the larger number of alternatively activated macrophages influences the persistence of the acute inflammatory cells and persistent parasite numbers remains unclear.

Given that collagen deposition is known to plateau, the intensity of the MT staining is indicative of the length of time that the fibroblasts had been actively laying down collagen. This allowed us to determine that the resistant C57BL/6 had been the first to clear its parasites and begin producing collagen, closely followed by the congenic mice. The susceptible BALB/c had little collagen deposition within the infected area indicating that the wound healing process was impaired. Whether the lack of alternatively activated macrophages during the later stages influences the fibroplasia remains to be determined.

In conclusion, this study establishes the importance of the leishmaniasis susceptibility loci *lmr1–3* in determining disease severity in the low dose metacyclic promastigotes–ear model of cutaneous leishmaniasis and shows a combined role for the localized cytokine response and cellular recruitment process in determining the outcome of infection in the skin. In addition, it shows for the first time that distinct mechanisms control the local vs. the systemic ability to eliminate infection.

ACKNOWLEDGEMENTS

We thank Lynn Buckingham and Gabriella Panoschi for technical assistance. This work was supported by grants from the US National Institutes of Health, the Australian National Health and Medical Research Council, the Howard Hughes Medical Institute, and the World Health Organization Special Program for Research and Training in Tropical Diseases (TDR).

REFERENCES

1 Sacks D & Noben-Trauth N. The immunology of susceptibility and resistance to *Leishmania major* in mice. *Nat Rev Immunol* 2002; **2** (11): 845–858.

2 McMahon-Pratt D & Alexander J. Does the *Leishmania major* paradigm of pathogenesis and protection hold for New World cutaneous leishmaniases or the visceral disease? *Immunol Rev* 2004; **201**: 206–224.

3 Baldwin T, Elso C, Curtis J, Buckingham L & Handman E. The site of *Leishmania major* infection determines the disease severity and immune responses. *Infect Immun* 2003; **71**: 6830–6834.

4 Roberts LJ, Baldwin TM, Curtis JM, Handman E & Foote SJ. Resistance to *Leishmania major* is linked to the H2 region on chromosome 17 and to chromosome 9. *J Exp Med* 1997; **185**: 1–6.

5 Roberts LJ, Baldwin TM, Speed TP, Handman E & Foote SJ. Chromosomes X, 9, and the H2 locus interact epistatically to control *Leishmania major* infection. *Eur J Immunol* 1999; **29** (9): 3047–3050.

6 Elso C, Kumar B, Smyth GK, Foote SJ & Handman E. Dissociation of disease susceptibility, inflammation and cytokine profile in *lmr1/2* congenic mice infected with *Leishmania major*. *Genes Immunity* 2004; **5**: 188–196.

7 Elso C, Roberts LJ, Smyth GK, *et al*. Leishmaniasis host response loci (*lmr1,2 and 3*) modify disease severity through a Th1/Th2 independent pathway. *Genes Immunity* 2004; **5**: 93–100.

8 Belkaid Y, Kamhawi S, Modi G, *et al*. Development of a natural model of cutaneous Leishmaniasis: powerful effects of vector saliva and saliva pre-exposure on the long-term outcome of *Leishmania major* infection in the mouse ear dermis. *J Exp Med* 1998; **188**: 1941–1953.

9 Belkaid Y, Mendez S, Lira R, Kadambi N, Milon G & Sacks D. A natural model of *Leishmania major* infection reveals a prolonged 'silent' phase of parasite amplification in the skin before the onset of lesion formation and immunity. *J Immunol* 2000; **165** (2): 969–977.

10 Nicolle CH. Cultures des corps de Leishman isoles de la rate dans trois cas d'anemic splenique infantile. *Bull Soc Pathol Exot* 1908; **1**: 121.

11 Courret N, Prina E, Mougneau E, *et al*. Presentation of the Leishmania antigen LACK by infected macrophages is dependent upon the virulence of the phagocytosed parasites. *Eur J Immunol* 1999; **29** (3): 762–773.

12 Sacks DL & da Silva RP. The generation of infective stage *Leishmania major* promastigotes is associated with the cell-surface expression and release of a developmentally regulated glycolipid. *J Immunol* 1987; **139** (9): 3099–3106.

13 Mitchell GF. Murine cutaneous leishmaniasis: resistance in reconstituted nude mice and several F1 hybrids infected with *Leishmania tropica major*. *J Immunogenetics* 1983; **10**: 395–412.

14 Parks DR, Bryan VM, Oi VT & Herzenberg LA. Antigen-specific identification and cloning of hybridomas with a fluorescence-activated cell sorter. *Proc Natl Acad Sci USA* 1979; **76**: 1962–1966.

15 Handman E & Hocking RE. Stage-specific, strain-specific, and cross-reactive antigens of *Leishmania* species identified by monoclonal antibodies. *Infect Immun* 1982; **37**: 28–33.

16 Sakthianandeswaren A, Elso CM, Simpson K, *et al*. The wound repair response controls outcome to cutaneous leishmaniasis. *Proc Natl Acad Sci USA* 2005; **102** (43): 15551–15556.

17 Cohen IK & Mast BA. Models of wound healing. *J Trauma* 1990; **30** (12 Suppl.): S149–S155.

18 Dovi JV, He LK & DiPietro LA. Accelerated wound closure in neutrophil-depleted mice. *J Leukoc Biol* 2003; **73** (4): 448–455.
19 Bennett NT & Schultz GS. Growth factors and wound healing: Part II. Role in normal and chronic wound healing. *Am J Surg* 1993; **166** (1): 74–81.
20 Gillitzer R & Goebeler M. Chemokines in cutaneous wound healing. *J Leukoc Biol* 2001; **69** (4): 513–521.
21 Holscher C, Arendse B, Schwegmann A, *et al*. Impairment of alternative macrophage activation delays cutaneous leishmaniasis in nonhealing BALB/c mice. *J Immunol* 2006; **176**: 1115–1121.

